Effect of Temperature on Surface Processes at the Pt(111)−Liquid Interface: Hydrogen Adsorption, Oxide Formation, and CO Oxidation

N. M. Marković,*,† T. J. Schmidt,‡ B. N. Grgur,† H. A. Gasteiger,‡ R. J. Behm,‡ and P. N. Ross†

Materials Sciences Division, Lawrence Berkeley National Laboratory, University of California, Berkeley, California 94720, and Abteilung Oberflachenchemie und Katalyse, Universitat Ulm, D-89069 Ulm, Germany

Received: June 3, 1999; In Final Form: July 20, 1999

The variation of the adsorption pseudocapacitance with temperature is used to obtain the enthalpy, entropy, and free energies of adsorption of H_{upd} and OH_{ad} on Pt(111) as a function of pH and nature of the anion of the supporting electrolyte. It is shown that the heat (enthalpy) of adsorption of hydrogen on Pt(111) at the electrochemical interface is essentially independent of either the pH of the electrolyte or the nature of the supporting anion. The heat of adsorption has a linear decrease with Θ_{Hupd}, from ~42 kJ/mol at $\Theta_{Hupd} = 0$ ML to ~24 kJ/mol at $\Theta_{Hupd} = 0.66$ ML. The heat of adsorption of OH_{ad} is more sensitive to the nature of the anion in the supporting electrolyte. This is presumably due to coadsorption of the anion and OH_{ad} in electrolytes other than the simple alkali bases. From the isosteric heat of adsorption of OH_{ad} in alkaline solution (ca. ~200 kJ/mol) and the enthalpy of formation of $OH^{\bullet}$ we estimated the Pt(111)−OH_{ad} bond energy of 136 kJ/mol. This value is much smaller than the Pt−O_{ad} bond energy at a gas−solid interface (~350 kJ/mol). In basic solution the electrooxidation of CO proceeds at low overpotentials (<0.2 V) between the adsorbed states of CO_{ad} and OH_{ad}, the latter forming at low overpotentials selectively at defect sites. In acid solution, however, these sites are not active because they are blocked by specific adsorption of anions of the supporting electrolyte.

1. Introduction

The past 2 decades have witnessed substantial advances in our knowledge of the electrocatalytic properties of well-defined platinum single-crystal surfaces. With the advent of surface structural probes such as ex situ analyses of emersed surfaces by low-energy electron diffraction (LEED),[1] in situ surface X-ray scattering (SXS), and in situ scanning tunneling microscopy (STM),[2] complemented by the development of the rotating ring-disk electrode technique for use of Pt(*hkl*) electrodes,[3] it became possible to establish the relationship between the surface structure and the electrocatalytic activity of Pt(*hkl*) electrodes. These methodologies present the ability to correlate the kinetics of the hydrogen and the oxygen electrode reactions with the structural sensitive adsorption of the reaction intermediates, such as underpotentially deposited hydrogen (hereafter, denoted as H_{upd}) and anions.[3−6] Measurements of the thermodynamic state functions for the H_{upd} state on Pt(111)[5,7] were recently obtained from the temperature dependence of voltammetric profiles of the Pt(111) surface in sulfuric acid solution. However, these experiments offered very little information about the oxygenated species, such as OH_{ad} or surface "oxide" because their formation on the Pt(111) surface is almost completely inhibited by the strong adsorption of bisulfate anions. To learn more about the kinetic and thermodynamic aspects of oxygenated species on Pt(111), the adsorption of these species should be studied in solutions with weakly adsorbing anions. Measurements in alkaline solution and perchloric acid solution would be of particular interest, since in these electrolytes the initial stage of the reversible surface adsorption of OH_{ad} has been clearly separated from an irreversible "oxide" formation. Much discussion has centered on the distinction between these two oxygenated species,[8] but there is general uncertainty about what physical processes are associated either with adsorption of OH_{ad} or with the "oxide" formation.

In this communication, we present voltammetric profiles of the Pt(111) surface in 0.1 M $HClO_4$ and 0.1 M NaOH obtained at different temperatures with the objective of observing the effect of temperature on the reversible adsorption of both the H_{upd} state and the OH_{ad} state, from which thermodynamic state functions may be obtained, and on the irreversible "oxide" formation process. The enthalpy of formation of the H_{upd} state on Pt(111) in 0.1 M $HClO_4$ and 0.1 M NaOH is derived from H_{upd} isotherms at variable temperatures. The chemisorption bond energy of the OH_{ad} state is estimated from the temperature dependence of the peak potential for OH_{ad} layer formation with respect to the O_2/H_2O reversible potential. The potential for incipient formation of the OH_{ad} state is estimated by titration using the electrooxidation of dissolved CO (denoted as CO_b). From this potential, the Pt(111)−OH_{ad} bond is estimated to be ca. −136 kJ/mol. This incipient adsorption of OH_{ad} is hypothesized as forming at steplike imperfections in the (111) surface.

2. Experimental Section

The pretreatment and assembly of the Pt(*hkl*) single crystals (0.283 cm^2) in a rotating disk electrode (RDE) configuration were fully described in our previous paper.[3] Following flame annealing, the single crystal was mounted in the disk position

* Corresponding author. E-mail: nmmarkovic@lbl.gov.
† University of California, Berkeley.
‡ Universitat Ulm.

10.1021/jp991826u CCC: $18.00
Published on Web 09/16/1999

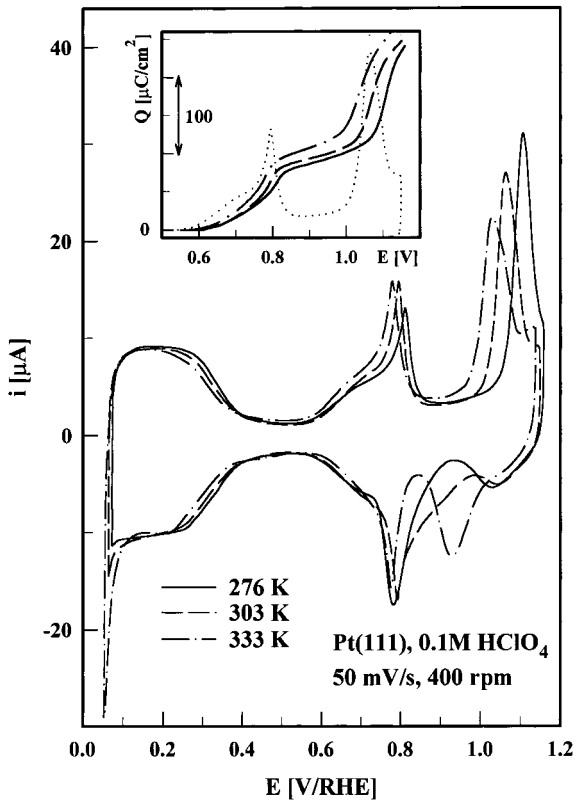

Figure 1. Cyclic voltammograms of Pt(111) in the RDE configuration in 0.1 M $HClO_4$ at various temperatures. Inset: Plot of charge associated with the reversible and irreversible oxide formation at various temperatures.

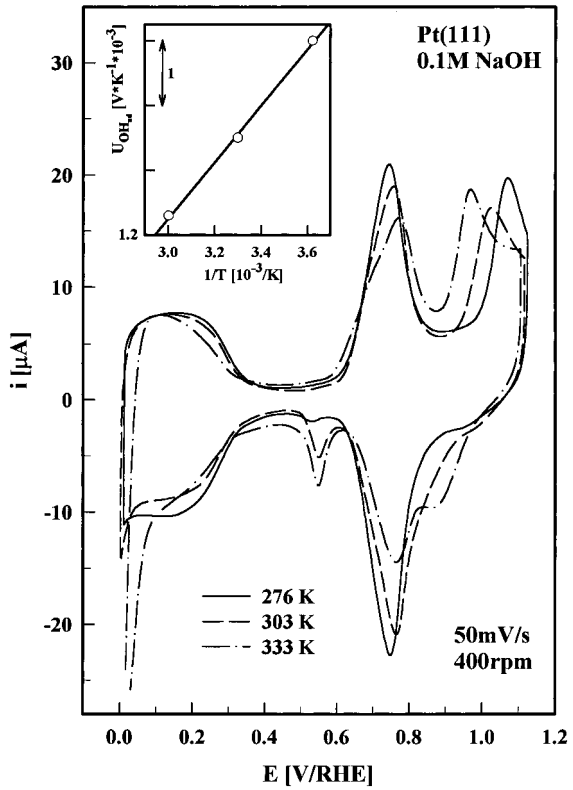

Figure 2. Cyclic voltammograms of Pt(111) in the RDE configuration in 0.1 M NaOH at various temperatures. Inset: Plot of U_{OHad}/T vs $1/T$.

of an insertible ring disk electrode assembly. Subsequently, it was transferred into a standard electrochemical cell and immersed in 0.1 M $HClO_4$ and 0.1 M NaOH under potentiostatic control at ~0.2 V. All experimental measurements reported in this study were conducted in a standard three-compartment electrochemical cell equipped with a water jacket. A circulating constant-temperature bath (Fisher Isotemp Circulator) maintained the temperature of the electrolyte within ±0.5 °C. For *every* temperature the crystal was reannealed, and after immersion the second sweep was recorded. In the study of CO_b electrooxidation, the solution was purged with pure CO gas (4 N CO purchased from Matheson) for 5 min while the electrode potential was held at 0.05 V, before potentiodynamic measurements were performed. The reference electrode was a saturated calomel electrode at 298 K separated by an electrolyte bridge. However, all potentials are referenced to the reversible hydrogen electrode (RHE) measured in the same solution at each temperature.[5]

In this work, the fractional coverages for H_{upd}, OH_{ad}, and "oxide" formation are based on the surface atomic densities and derived assuming one electron transfer per Pt surface atom. The surface atomic density of the Pt(111) was based on the unreconstructed (1 × 1) geometry present in contact with several electrolytes (1.5×10^{15} atoms/cm^2).[3−6] The theoretical charge for one monolayer of H_{upd} and OH_{ad} would be 240 μC/cm^2 for the Pt(111)-(1 × 1) surface.

3. Results

3.1. Temperature Effects on Cyclic Voltammery of Pt-(111) in 0.1 M $HClO_4$ and 0.1 M NaOH. A close inspection of Figures 1 and 2 reveals that voltammetric features recorded within the temperature range 276−333 K are very similar to those observed at room temperature in the same electrolytes.[9] Given that consensus in interpretation appears to be emerging with respect to the nature of processes that occur on Pt(111) in 0.1 $HClO_4$ and 0.1 M NaOH at ambient temperature, only a brief interpretation of voltammograms in Figures 1 and 2 will be presented in this section. Current−potential curves of Pt-(111) in both electrolytes give four distinctive potential regions. Starting from the negative potential limit, a broad H_{upd} potential region (~$0.05 < E < 0.375$ V) is followed first by a so-called "double-layer" potential region, then with the reversible formation of the OH_{ad} layer (the so-called "butterfly" feature, $0.6 < E < 0.85$ V), and finally with the irreversible "oxide" formation potential region (~$E > 1.1$ V).

3.1.1. H_{upd} Region. Current−potential curves for Pt(111) in Figures 1 and 2 give distinctive voltammograms with broad, nearly flat H_{upd} peaks in both 0.1 M $HClO_4$ and 0.1 M NaOH. Depending on the pH of the solution, the H_{upd} state on the Pt-(111) surface is generated in surface reactions either from protons or from water molecules:

$$Pt + H_3O^+ + e^- = Pt{-}H_{upd} + H_2O \qquad (pH \lesssim 7) \quad (1)$$

$$Pt + H_2O + e^- = Pt{-}H_{upd} + OH^- \qquad (pH \gtrsim 7) \quad (2)$$

Irrespective of the pH of the solution, the thermodynamic state functions can be obtained in an unambiguous way from the experimentally measured temperature dependence of the H_{upd} adsorption isotherms referenced to the potential of the $(^1/_2)H_2/H^+$ electrode, E_{rhe}, in the same electrolyte at the same temperature.[10]

Adsorption isotherms, Θ vs E, were obtained by integrating the anodic charge under the underpotential (UPD) voltammetry peaks. The apparent Gibbs energy of adsorption, $\Delta G_{H_{upd}}(\Theta)$, was obtained as a function of coverage at each temperature by

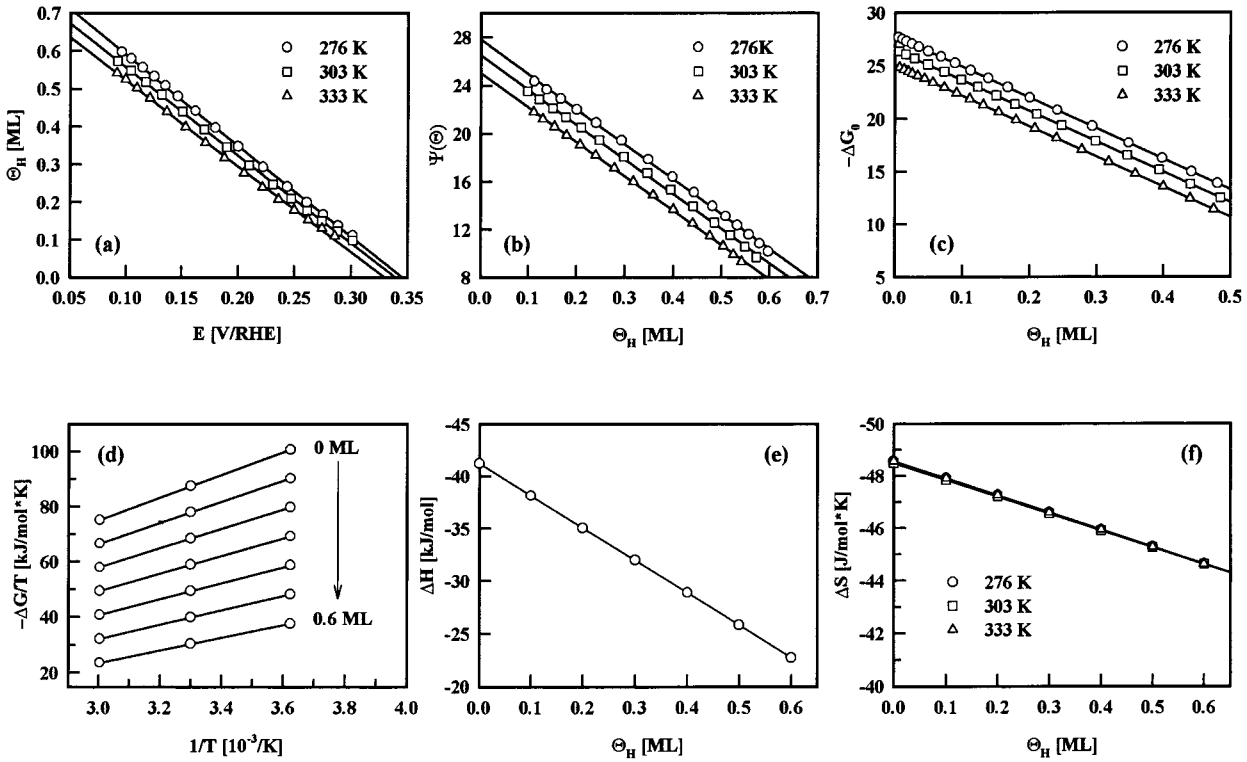

Figure 3. Adsorption isotherms (a) and thermodynamic functions (b−f) for H_{upd} on Pt(111) in 0.1 M $HClO_4$ at 276, 303, and 333 K. For details see text. Note: $\Psi = RT\ln[\theta/(1-\theta)] + E_{rhe}F = -\Delta G^0_{H_{upd}} - r\theta$.

fitting these isotherms to a generalized (nonideal) form of the Langmuir isotherm assuming first-order kinetics:[11]

$$\frac{\Theta}{1-\Theta} = \exp\left(-\frac{E_{rhe}F}{RT}\right)\exp\left(-\frac{\Delta G_{H_{upd}}(\Theta)}{RT}\right) \qquad (3)$$

As we found before[5] in sulfuric acid solution, the isotherms are essentially linear over a wide range of coverage, meaning that they are well-fit by a Temkin−Frumkin isotherm,[11] which is a special case of eq 3, where the Gibbs energy of adsorption is assumed to vary linearly with coverage,

$$\Delta G_{H_{upd}} = \Delta G^{\Theta=0}_{H_{upd}} + r\Theta \qquad (4)$$

Substitution in eq 3 produces

$$\frac{\Theta}{1-\Theta}\exp\left(\frac{r\Theta}{RT}\right) = \exp\left(-\frac{E_{rhe}F}{RT}\right)\exp\left(-\frac{\Delta G^{\Theta=0}_{H_{upd}}}{RT}\right) \qquad (3a)$$

and $\Delta G^{\Theta=0}_{H_{upd}}$ is the initial (zero coverage) free energy of adsorption. Equation 3 produces a linear Θ vs E relation for intermediate values of Θ, since the term $\Theta/(1-\Theta) \approx 1$ and varies much more slowly with E than the exponential terms. The interaction parameter f ($=r/(RT)$) is repulsive for $f > 0$ and attractive for $f < 0$ and characterizes the lateral interaction in the H_{upd} adlayer. The apparent free energy of adsorption at any given temperature is then characterized by just two parameters, $\Delta G^{\Theta=0}_{H_{upd}}$ and f, both of which can be obtained by simple curve fitting. The isosteric heats of adsorption can be obtained from the temperature dependence of the Gibbs free energy of adsorption from the relation

$$q^H_{st} = -\frac{\partial(\Delta G_{H_{upd}}/T)_\theta}{\partial T^{-1}} \qquad (5)$$

TABLE 1: Thermodynamic State Functions for H_{Upd} in (a) 0.1 M NaOH, (b) 0.1 M $HClO_4$, and (c) 0.05 M H_2SO_4, Evaluated Using Eq 3a (See Also Figures 3 and 4)

T [K]	$\Delta G^{\Theta=0}_{H_{upd}}$ [kJ/mol]	$f = r/(RT)$	$\Delta H_{H_{upd}}$ [kJ/mol]	$\Delta S_{H_{upd}}$ [J mol^{-1} K^{-1}]	D_{Pt-H} [kJ/mol]
		(a) In 0.1 M NaOH			
276	−24	16	−41	∼−63	∼240
303	−22	15			
333	−20	13			
		(b) In 0.1 M $HClO_4$			
276	−28	13	−42	∼−45	∼240
303	−27	12			
333	−25	10			
		(c) In 0.05 M H_2SO_4			
276	−29	14	−42	∼−48	∼240
303	−28	13			
333	−27	11			

and the entropy of adsorption from the relation

$$\Delta S_{H_{upd}} = -\frac{\partial(\Delta G_{H_{upd}})_\Theta}{\partial T^{-1}} \qquad (6)$$

The resulting values (Θ = 0) of $q^H_{st} = -\Delta H_{H_{upd}}$, $\Delta S_{H_{upd}}$, $\Delta G^{\Theta=0}_{H_{upd}}$, f, and the D_{M-H} bond energies for all three different electrolytes are calculated from the curves in Figures 3 and 4 and summarized in Table 1. The values are virtually identical *in all three solutions, independent of the anion or the pH*. In all electrolytes, the apparent Gibbs energy of adsorption for the H_{upd} state on Pt(111) has a linear decrease with the coverage, from about -24 ± 4 kJ/mol extrapolated at $\Theta = 0$ to about -14 ± 2 kJ/mol at $\sim\Theta \cong 0.66$ ML (1 ML = 1 H_{upd} per Pt), which is the saturation coverage (for $p_{H_2} = 1$ atm). The best-fit values of the Frumkin parameter, f, which characterizes the lateral repulsive interaction in the hydrogen adlayer, are relatively high, $f = 10.5-13$, over the temperature range 276−

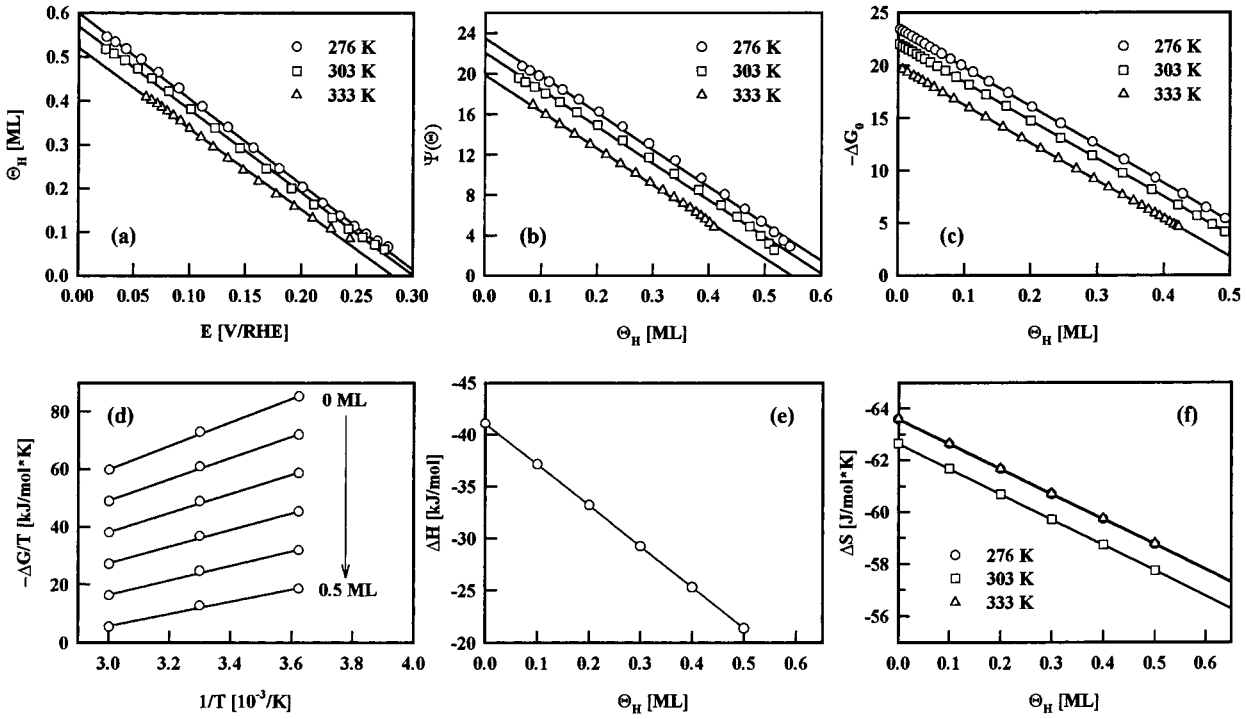

Figure 4. Adsorption isotherms (a) and thermodynamic functions (b−f) for H_{upd} on Pt(111) in 0.1 M NaOH at 276, 303, and 333 K. For details see text. Note: $\Psi = RT \ln[\theta/(1-\theta)] + E_{rhe}F = \Delta G^0_{H_{upd}} - r\theta$.

333 K, suggesting a strong lateral repulsion between H_{upd} species adsorbed *on* the Pt(111) surface.[5] This lateral repulsion causes the Pt−H_{upd} bond energy to decrease so significantly with increasing coverage that the saturation coverage is much less than 1 H_{upd} per Pt, only 0.66 H_{upd} per Pt, in the UPD potential region, i.e., equivalent to H_2 partial pressures of ≤1 atm.

A fundamental measure of interest for the Pt(111)−H_{upd} system is the Pt−H_{ad} bond energy, D_{M-H}, corresponding to the dissociation reaction

$$Pt{-}H_{ad} = Pt + H^{\bullet} \tag{7}$$

where H_{ad} refers to hydrogen adsorbed at either the electrochemical or the gas−solid interface and H• to atomic hydrogen. D_{M-H} may be obtained from the isosteric heat of adsorption by the relation

$$D_{M-H} = (^1/_2)[q^H_{st} + D_{H-H}] \tag{8}$$

where D_{H-H} is the dissociation energy of the H_2 molecule (∼435 kJ/mol) and q^H_{st} is the isosteric heat of adsorption at constant pressure, which has its usual definition as the apparent enthalpy of adsorption, e.g., $q^H_{st} = \Delta H_{H_{ad}}$. When eq 8 is adopted, the resulting values of the Pt(111)−H_{upd} bond energies in alkaline and acid solutions are found to be within 240−250 kJ/mol, reflecting that D_{M-H} is *independent* of the pH of solution.

3.1.2. Reversible OH Region. The H_{upd} region observed in the potentiodynamic sweep voltammetry of Figures 1 and 2 is followed at more positive potentials first by a (nominally) "double-layer" potential region, where the current flows only from charging of the double-layer, and then the potential region of the so-called "butterfly" feature. The physical process(es) that are associated with the "butterfly" feature have been the subject of controversy for some time (see refs 8, 13, 14 for overviews from different perspectives). There is some consensus for the interpretation that in alkaline solution the pseudocapacitance observed in the cyclic voltametry of Pt(111) in the range $0.6 < E < 0.85$ is due to reversible formation of an OH_{ad} layer,[8,14] which presumably is just OH^- adsorption with charge transfer,

$$OH^- + Pt = Pt{-}OH_{ad} + e^- \tag{9}$$

One observation evident from Figures 1 and 2 is that the "butterfly" feature occurs at the same potential with respect to the RHE in NaOH and $HClO_4$ solutions. This would imply that the "butterfly" feature in $HClO_4$ is also associated with the adsorption of OH_{ad}. On the basis of the monolayer oxide film formation in acid solution, it is reasonable to suggest that the OH_{ad} adsorption in $HClO_4$ proceeds according to

$$2H_2O + Pt = Pt{-}OH_{ad} + H_3O^+ + e^- \tag{10}$$

Temperature-dependent features of OH_{ad} adsorption seen in Figures 1and 2 can be summarized as follows. (a) While the sharp 'butterfly" peak in perchloric acid solution is shifted negatively with increasing the temperature, in alkaline solution the "butterfly" peak is shifting positively over the same temperature range. (b) The shape of the butterfly feature in $HClO_4$ is not significantly affected by increasing the temperature; it tends to become broader, however, with higher temperatures in NaOH. (c) The "oxide" formation/reduction process at $E > 0.9$ V becomes more reversible as the temperature is increased to 333 K. At 333 K it is clear that the standard potential ($E°$) for the formation of "oxide" is close to 1.0 V. This is an important value, as we will demonstrate below in the thermodynamic analysis. (d) Although the initial reduction of oxide is similar in $HClO_4$ and NaOH, the complete reduction of both reversible and irreversible states of oxide appears to be different in these two electrolytes. At higher temperatures in NaOH, upon sweeping negatively from 1.15 V, the charge for the reduction process is widely distributed in potential, from 0.95 V all the way to ca. 0.3 V

The thermodynamic analysis of the temperature dependence of the current−potential curves for the OH_{ad} adsorption process is not as straightforward as for the H adsorption process. In particular, in 0.1 M $HClO_4$ the energetics of the Pt(111)−OH_{ad} state is influenced by coadsorption of Cl^- anions,[13] and therefore, the apparent thermodynamic functions cannot be evaluated by analyzing isotherms recorded at various temperatures. On the other hand, although the reversible adsorption of OH_{ad} in alkaline solution is not accompanied by the concomitant adsorption of anions, thermodynamic quantities for the reversible adsorption of OH cannot be evaluated accurately because of the lack of a clearly defined reference potential of thermodynamical data for gas-phase adsorption of these species. The analysis we use here is that first suggested by Ross.[15] Analogous to the definitions customarily used for H_{ad} and (in the gas phase) O_{ad}, we use H_2(gas) and O_2(gas) at standard potential (STP) as the reference states and define the apparent Gibbs energy of adsorption of OH_{ad}, $\Delta G_{OH_{ad}}^{\Theta=0.5}$, as the Gibbs energy of the reaction

$$H_{2(gas)} + O_{2(gas)} + 2Pt = 2Pt{-}OH_{ad} \qquad (11)$$

The standard state for OH_{ad} is taken to be a coverage of 0.5 ML, since it is the custom for adsorption isotherms at the solid liquid interface.[10,11] The free energy of formation of the bulk "oxide", which we assume to be $Pt(OH)_2$, will then be given by the directly comparable reaction

$$H_{2(gas)} + O_{2(gas)} + Pt = Pt(OH)_2 \qquad (12)$$

The free energy for this reaction is not known. The NBS compilation by Wagman et al.[16a] gives a standard *enthalpy* of formation, $\Delta_f H^0$, of −351.9 kJ/mol. By use of the standard entropies of formation of the transition metal dihydroxides, $M(OH)_2$, with M = Fe, Co, Ni, for which $-T\Delta_f S^0 \approx 80-85$ kJ/mol,[16a] the estimated value for the Gibbs energy of formation of the bulk "oxide" at 298 K is ca. −230 kJ/mol. The estimated standard potential, $E°$, for the electrode reaction for bulk oxide formation

$$2H_2O + Pt = Pt(OH)_2 + 2H^+ + 2e^- \qquad (13)$$

is then ca. 1.0 ± 0.05 V (RHE). The validity of this estimate is based on the observation that the entropy of formation of solids such as metal oxides or hydroxides depends primarily on the change in the degrees of freedom of the gaseous reactants (oxygen or water) and is relatively independent of the metal.[16b] Note that this standard potential is independent of pH when the RHE is used as a reference electrode. This standard potential of >0.9 V for $Pt(OH)_2$ formation is consistent with the assignment of the irreversible state as a bulklike "oxide" chemically related to $Pt(OH)_2$.

In the case of oxygen adsorption on metals in the gas phase, the adsorbed state of oxygen may or may not be thermodynamically favored over the bulk oxide, i.e., adsorbed oxygen may be either endothermic or exothermic with respect to the bulk oxide.[17] For transition metals, it is typically the case that the initial heat of adsorption of oxygen is more exothermic than the heat of formation of the most stable bulk oxide.[17] From these general considerations, we might expect, therefore, that the enthalpy of adsorption of OH_{ad} is exothermic relative to the "oxide" and thus is more negative than −230 kJ/mol. Correspondingly, the standard potential for the adsorption reaction 11 should be less than 1.0 V (RHE), consistent with our assignment of the "butterfly" feature as OH_{ad}.

To analyze the temperature dependence of the peak positions for OH_{ad}, and thereby extract thermodynamic functions such as the isosteric heat of adsorption, it is convenient to define a potential function U,

$$U_{OH_{ad}} = E^0_{O_2/H_2O} - E^0_{OH_{ad}} \qquad (14)$$

where $E^0_{O_2/H_2O}$ is the standard potential for the oxygen evolution reaction (OER) for each temperature,

$$H_2O = \frac{1}{2}O_2 + 2H^+ + 2e^- \qquad (15)$$

and $E^0_{OH_{ad}}$ is the standard potential for the adsorption reaction given by eq 11. The advantage of using the potential difference in eq 14 is that this difference is independent of the reference electrode being used and of the pH of the electrolyte. Experimentally, we will use the difference between the potential of the peak in the OH_{ad} feature of the voltammetry curves and the (calculated) value of $E^0_{O_2/H_2O}$ as a function of temperature. The most important thermodynamic function to be extracted from the temperature-dependent potentials is the isosteric heat of adsorption of OH_{ad}, which is defined as

$$q_{st}^{OH} = -\frac{\partial(\Delta G_{OH_{ad}}/T)_\theta}{\partial T^{-1}} \qquad (16)$$

The derivative in eq 16 is taken at constant coverage of $\Theta_{OH_{ad}}$. Experimentally, we are using the peak potentials in the voltammetry curves, for which $\Theta_{OH_{ad}}$ is approximately constant with temperature and corresponds to a coverage of about 0.5 ML.

We can substitute eq 14 into eq 16 and rewrite it as

$$q_{st}^{OH} = \frac{\partial[F(U_{OH_{ad}}/T)_\Theta - (\Delta G^0_{O_2/H_2O}/T)]}{\partial T^{-1}} \qquad (17)$$

Note that the second term in this derivative is, by definition, just the standard enthalpy of formation of water ($\Delta_f H^0_{H_2O}$ = −285.8 kJ/mol) so that eq 17 becomes

$$q_{st}^{OH} = F\frac{\partial(U_{OH_{ad}}/T)_\theta}{\partial T^{-1}} - \Delta_f H^0_{H_2O} \qquad (18)$$

The experimental values for the function $U_{OH_{ad}}/T$ are shown in the inset in Figure 2. The slopes of this function for 0.1 M NaOH is −0.88 V, and the isosteric heat of adsorption for OH_{ad} on Pt(111) is then ca. 200 kJ/mol. The fact that the position of the "butterfly" feature is the same in alkaline and acid solution (vs RHE) may suggest that the isosteric heat of adsorption for OH_{ad} on Pt(111) is *independent* of pH of solution, as was the case for the isosteric heat of adsorption for H_{upd} (see section 3.1.2).

As with UPD hydrogen, it is of interest to compare the adsorbate bond energy at the electrochemical interface to that of the same bond at the gas-phase interface where possible. To do that, we need to extract the Pt−OH_{ad} bond energy (D_{M-OH}) from q_{st}^{OH} using the following Born−Haber cycle:

$$H_{2(gas)} = 2H^\bullet \qquad \Delta_f H^0_{H_2} = +D_{H-H} \qquad (a)$$

$$O_{2(gas)} = 2O^\bullet \qquad \Delta_f H^0_{O_2} = +D_{O-O} \qquad (b)$$

$$2H^{\bullet} + 2O^{\bullet} = 2OH^{\bullet} \qquad \Delta_r H^0 = 2\Delta_f H^0_{OH\bullet} - D_{H-H} - D_{O-O} \tag{c}$$

$$2OH^{\bullet} + 2M = 2M-OH_{ad} \qquad \Delta_f H^0_{M-OH} = -2D_{M-OH} \tag{d}$$

Thus, the enthalpy change of the overall reaction

$$H_{2(gas)} + O_{2(gas)} + 2M = 2M-OH_{ad} \qquad \Delta_r H^0_{M-OH} = -q^{OH}_{st} \tag{19}$$

is the sum of all the individual enthalpies, so

$$-q^{OH}_{st} = 2\Delta_f H^0_{OH\bullet} - 2D_{M-OH} \tag{20}$$

and finally, the $M-OH_{ad}$ bond energy from the experimental value of q^{OH}_{st} and the enthalpy of formation of $OH^{\bullet}$, $\Delta_f H^0_{OH\bullet}$ ($\Delta_f H^0_{OH\bullet} = +38.95$ kJ/mol), can be calculated from

$$D_{M-OH} = \frac{1}{2}q^{OH}_{st} + \Delta_f H^0_{OH\bullet} \tag{21}$$

Using the value of q^{OH}_{st} from alkaline solution and the value of $\Delta_f H^0_{OH\bullet}$ from Wagman et al.,[16a] we estimate the $M-OH_{ad}$ bond energy on Pt(111) to be ca. 136 kJ/mol. Note that the corresponding value of the $Pt-O_{ad}$ bond energy would be given by the relation

$$D_{M-O} = \frac{1}{2}[q^{O}_{st} + D_{O-O}] \tag{22}$$

where q^{O}_{st} is the isosteric heat of adsorption of oxygen and D_{O-O} is the dissociation energy of O_2 molecule ($D_{O_2} = 488$ kJ/mol[18]). Values for q^{O}_{st} for Pt(111) are well-established at the gas−solid interface,[19] ca. 190−210 kJ/mol, so that the $M-O_{ad}$ bond energy at the gas−solid interface is $D_{M-O} = 350$ kJ/mol. Wagman et al. also list an enthalpy of formation of the gaseous dioxide, PtO_2, from which we can estimate a "bulk" Pt−O bond energy of 163 kJ/mol. As expected, the surface Pt−O bond is significantly stronger than the bulk bond, consistent with the resistance of Pt to bulk oxidation in oxidizing atmospheres, yet having a high activity as an oxidation catalyst.

3.1.3. Irreversible OH Region. When the positive potential limit is more positive than 0.85 V, the surface oxidation/reduction process becomes irreversible, as seen from the separation of the anodic and cathodic peaks. This irreversible state is commonly referred to as surface "oxide", although the physical nature of this state is not actually known but is most likely chemically related to $Pt(OH)_2$.[20] The irreversibility of oxide formation/reduction implies that the process does not proceed at quasi-equilibrium, and therefore, thermodynamic state functions for the "oxide" state cannot be obtained from the temperature dependence of the current−potential data. Temperature effects on the "oxide" formation, however, may provide some additional information that can help us to develop a more detailed understanding of the monolayer oxide formation on Pt(111) in acid and alkaline solutions. Figures 1 and 2 reveal that when the temperature is raised from 276 to 333 K, the peak shapes and positions for oxide formation/reduction in $HClO_4$ and NaOH respond differently. The peak height for the formation of the oxide clearly tends to decrease at higher temperatures in both electrolytes; however, the peak for the oxide formation on Pt(111) in 0.1 $HClO_4$ is much sharper than in 0.1 M NaOH. The sharper peak for oxide formation in $HClO_4$ is attributed to the effect of adsorbed Cl^- and its coadsorption with and/or displacement by the oxygenated species.[21,22] Recent surface X-ray scattering (SXS) results[21,22] indicate the coadsorption of Cl^- facilitates the place-exchange between the platinum atoms and oxygenated species, which accounts for the increased sharpness of the peak and the increased reversibility as the temperature is raised to 333 K (relative to NaOH). Although the initial reduction of oxide is similar in $HClO_4$ and NaOH, the complete reduction of both reversible and irreversible states of oxide appears to be different in these two electrolytes. While in perchloric acid solution the reduction of oxide seems to be completed at 0.6 V, the complete reduction of oxygenated species in alkaline solution takes place at more negative potentials. A small peak at 0.55 V is clearly resolved in the cyclic voltammetry of Pt(111) in NaOH, whose intensity increases as the temperature is raised; this peak appears only when the potential limit is above 0.85 V and thus is coupled directly to reduction of the irreversible (oxide) state. It is also interesting to note that at higher temperatures in NaOH, upon sweeping negatively from 1.15 V, the charge for the reduction process is widely distributed in potential, from 0.95 V all the way to ca. 0.3 V. It appears that the later stage(s) of the oxide reduction process in NaOH actually becomes inhibited by increasing temperature.

3.2. Temperature Effects on CO_b Oxidation on Pt(111) in 0.1 M $HClO_4$ and 0.1 M NaOH. To get further insight into the adsorption of the OH_{ad} species at low potentials, the electrooxidation of dissolved CO_b was examined on Pt(111) in $HClO_4$ and NaOH. Markovic et al.[23] have recently reported a detailed study of this reaction in H_2SO_4, and our purpose here is to compare the behavior in NaOH with that in $HClO_4$ and/or H_2SO_4 (which are quite similar). We shall use the same terminology here as used there in describing the characteristic features. Figure 5 shows that two potential regions can be resolved in both electrolytes, i.e., a region of low rate of CO_b electrooxidation (termed the preignition region) and the transition to a high rate of CO_b electooxidation (above the ignition potential), where the current is diffusion-limited. Furthermore, Figure 5 clearly indicates much slower oxidation kinetics on Pt(111) in $HClO_4$ compared to that in NaOH. In the preignition potential region, it is slower by ca. 2 orders of magnitude, and in the ignition potential region it is shifted anodically by ca. 0.4 V for perchloric acid solution. The fact that the ignition potential in $HClO_4$ is shifted positively from that in NaOH is further support for the supposition that the adsorption of OH_{ad} at 0.6 V in $HClO_4$ is inhibited by Cl^- anions present in "pure" perchloric acid (as it is in H_2SO_4 by sulfate anion adsorption). It is surprising, however, that the onset of the preignition region in alkaline solution is observed even in the H_{upd} region (!), i.e., in the potential region below which OH_{ad} is not observed in the base voltammetry. It is also important to note that the currents for oxidation of CO_b in the preignition region in alkaline solution are *not* transient currents because if the potential sweep is stopped at any potential above 0.1 V, the steady-state current decays by only about 10%. On the other hand in either acid solution (H_2SO_4 or $HClO_4$), *only* transient currents are observed; i.e., if the potential sweep is halted below ca. 0.8 V, the current decays to an unmeasureably small value.

To gain more information on the catalytic mechanism of CO_b electrooxidation in alkaline solutions and the activation energy associated with this reaction, we measured the temperature dependence of the current at 0.3 V (the preignition region) and 0.6 (above the ignition potential), the latter corrected for diffusion. The apparent activation energies of CO oxidation in

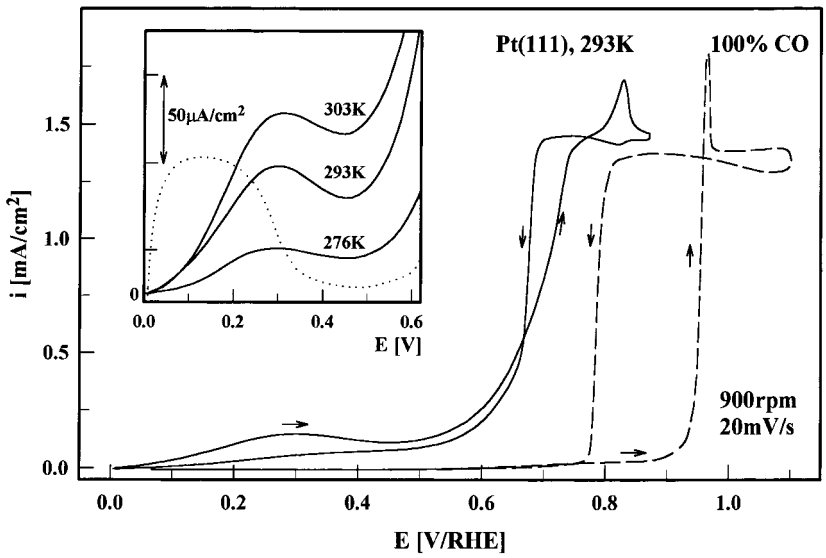

Figure 5. Current−potential curves for the electrooxidation of CO_b dissolved in NaOH (solid curve) and $HClO_4$ (dashed curve) on Pt(111) at 293 K. Inset: Magnification of the preignition region at various temperatures in NaOH. The dotted curve represents basic CV in CO-free solution (note: current scale only for CO oxidation).

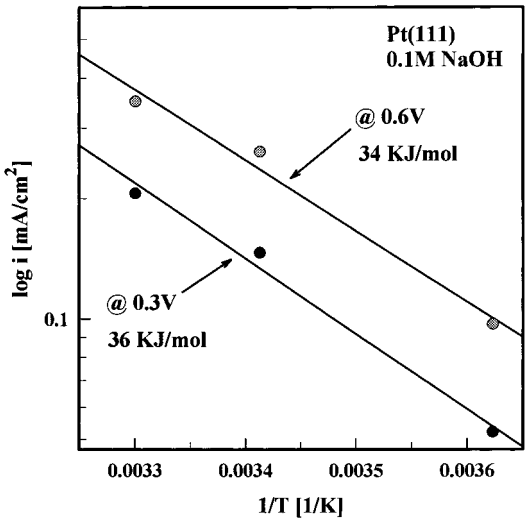

Figure 6. Arrhenius plots of log(*i*) vs 1/*T* for Pt(111) in 0.1 M NaOH at 0.6 and 0.3 V. Data taken from Figure 5.

the preignition region and above the ignition potential are shown in Figure 6. Arrhenius plots at 0.3 and 0.6 V yield activation energies of 36 and 34 kJ/mol, respectively. The close agreement between values for the activation energies at these two different potentials suggests that there is no fundamental difference in the reaction mechanism for CO oxidation in the preignition region and above the ignition potential. Since the ignition potential in NaOH lies exactly at the onset of the major OH_{ad} feature in the base voltammetry curve, the "ignition" corresponds to a dramatic increase in the OH_{ad} coverage. Thus, the distinction in rate between the two regions arises from the potential dependence of the coverage by OH_{ad}.

4. Discussion

4.1. Pt−H_{upd} Bond Energy. The values for the heat of adsorption of H_{upd} (the Pt(111)−H_{upd} bond energy) on Pt(111) at the electrochemical interface can be compared with previous values reported at this interface *and* with values for H adsorption on Pt(111) at the gas−solid interface. The Pt(111)−H_{upd} bond energy in Table 1 for sulfuric acid is essentially identical to that determined recently by Zolfaghari and Jerkiewiscz[7] using flame annealed crystals, as here, and in reasonable agreement with that reported many years earlier by Ross[15] using an ultrahigh vacuum (UHV) prepared LEED charactrized surface in perchloric acid. So a bond energy of 240 ±10 kJ appears to be a reliable value for the Pt−H_{upd} bond at the Pt(111)−electrolyte interface, in the limits of small coverages. This is well within the range of values reported in the latest compilations of adsorption energies for hydrogen on Pt(111) in UHV, where values range from 235 to 270 kJ.[24] In the early 60s Breiter has reported that the initial heats of adsorption of hydrogen on polycrystalline Pt were nearly identical in both environments.[25] The chemisorptive binding energy of H_{upd} and the thermodynamics of the Pt−H_{upd} state were also discussed in the early 70s by Conway and co-workers[10] and more recently in refs 5, 7, 26. It has also been shown by means of a Born−Haber cycle that such an outcome is expected if the interaction of water and the anion of the supporting electrolyte is sufficiently weak.[15] However, as we shall discuss further here, a "perfect" Pt(111) surface appears to satisfy these conditions, but defects on the (111) face and other low-index faces of Pt do not appear to, and produce a significant divergence between the electrochemical and the vacuum interface.

Many papers were written in the 1975−1988 period about the effect of defects in the Pt(111) surface on the Pt−H bond energy *at both interfaces*. Both the UHV and the electrochemical community used stepped (111) surfaces to investigate the role of defects. A comparison of the effect of step defects on the Pt−H bond energy at the two different interfaces produces an informative contrast. The low-coverage heat of H adsorption in UHV not only is surprisingly insensitive to defects in the (111) surface but also varies relatively little between the different low-index crystal faces.[19,24] The heat of adsorption is ca. 75−100 kJ/mol, and the Pt−H bond energy ca. 255−268 kJ, with steps on the (111) surface having ca. 10−15% higher bond energy than the flat terraces. The unreconstructed (1 × 1)-(110) surface has the highest Pt−H bond energy, consistent with chemical intuition that the most open (coordinatively unsaturated) surface would have the strongest adsorbate bonding. Masel and co-workers[19] have recently offered an explanation of the relatively small effect of Pt surface coordination number on the binding of hydrogen (and other small molecules) in terms of electronic "relaxation", i.e., a relaxation process that allows the

low-coordination atoms to gain electron density and become less coordinatively unsaturated electronically. Conceptually, this is the same as the idea of electronic "smoothing" of atomically rough surfaces articulated by Smoluchowski.[27]

At the electrochemical interface, however, the effect of defects in the (111) surface is profoundly different.[28−30] Rather than producing sites that bind hydrogen more strongly than the flat terraces, stepped surfaces appear to introduce a *more weakly bound state* of H_{upd}, regardless of step geometry, i.e., direction of miscut. In addition, the (110) surface appears to have the *weakest* $Pt-H_{UPD}$ bond energy, in direct contrast to the trend at the vacuum interface. In a separate work Markovic et al.[29] and Ross[30] reported similar effects of defects on the (111) surface voltammetry but interpreted the results differently from Clavilier and co-workers.[28] For example, Markovic et al.[29] proposed that bisulfate anions are more strongly adsorbed along (111)−(111) and/or (111)−(100) terrace-step sites than on the (111) terrace sites and that bisulfate desorption is concurrent with hydrogen adsorption. On the other hand, Ross invoked the local work function concept of Wandelt,[31] as applied by Alnot et. al.[32] to stepped (111) surfaces, to show that anions would be expected to adsorb at step sites at much lower potential, ca. 0.2−0.3 V, than "normal" adsorption on the terraces. Thus, the redistribution of charge in the voltammetry of (111) surfaces due to defects is *not* due to lower $Pt-H_{upd}$ binding at steps but to preferential adsorption of anions at steps. The coadsorption of anions with H_{upd} on the terraces has the expected repulsive effect of lowering the $Pt-H_{upd}$ bond energy on the terraces. To our knowledge, the interpretation presented by Ross has not been disputed or displaced by a more compelling one. In the context of the present study, we shall apply this concept of preferential anion adsorption at defects below to explain the dramatic differences in CO_b electroxidation behavior in different electrolytes.

4.2. Catalytic Properties of OH_{ad}. The remarkable effect of pH on the catalytic properties of the Pt(111) surface for the continuous oxidation of CO_b is not easily explained. The pronounced current plateau in the preignition region corresponds to a Langmuir−Hinshelwood type surface reaction between CO_{ad} and OH_{ad} in both acid and base solutions:

$$CO_{ad} + OH_{ad} = CO_2 + H^+ + e^- \qquad (23)$$

For the purpose of our discussion here we will focus on the reactant side of this elementary step. We consider, qualitatively, the contributions of the heat of adsorption of CO_{ad} and OH_{ad}, respectively, to the activation energy for reaction step 20 and the contribution of the electrode potential in determining (primarily) the surface coverage by OH_{ad}. The objective is to determine, at least qualitatively, where we might expect to see the pH play a major role.

Markovic et al.[23] suggested that the reaction pathway for CO_{ad} oxidation on Pt(111) in the preignition potential region in sulfuric acid solution occurs via a weakly bonded state created by the "crowding" of the surface with adsorbed CO that reduces its adsorption energy via CO−CO repulsion. This hypothesis presumes that in this potential region the rate is limited by the surface coverage of oxygen-containing species, that CO_{ad} prevents the adsorption of sufficient OH_{ad} for the reaction to proceed. The fact that the experimental apparent activation energy of 30−40 kJ/mol is relatively low supports this supposition. The rate of this reaction in acid solution depends on the delicate balance between the coverage of coadsorbed CO_{ad}, OH_{ad}, and a third party (spectator) species, viz., the adsorbed anions from the supporting electrolyte. In alkaline solution, the latter do not exist and anions of the supporting electrolyte are *reactants*, not *spectators*. We have seen from the thermodynamic analysis described above that in order to adsorb OH_{ad} on the (111) surface in the preignition potential region, OH_{ad} would have to be strongly adsorbed, about 0.4 V below the main adsorption at >0.6 V. This would translate into an increase in $Pt-OH_{ad}$ bond energy by ca. 70−80 kJ/mol, e.g., from 136 kJ/mol in the "butterfly" region to ca. 206−216 kJ/mol. We propose that the adsorption of OH_{ad} with this higher bond energy occurs at *defects* in the (111) surface. Two hypotheses can be invoked in order to describe a reaction mechanism of OH_{ad} adsorption at low potentials: (i) OH_{ad} can be adsorbed on the virgin Pt sites that are occupied neither by anions nor CO_{ad}, i.e., filling in holes of the CO_{ad} adlayer by OH_{ad}; (ii) at a high surface coverage by CO_{ad} adlayer, CO_{ad} may be displaced by OH_{ad} because the isosteric heat of adsorption of OH on Pt is relatively high (from our calculations ca. 200 kJ/mol), and given that the heat of adsorption of CO on Pt(111) in the gas phase decreases from 140 kJ/mol at $\theta_{CO} = 0$ to 45 kJ/mol at saturation coverages (see ref 23 and references therein), it is plausible that some CO_{ad} may be displaced by OH_{ad}. Furthermore, a comparison of the values for the $Pt(111)-OH_{ad}$ bond energies with the $M-O_{ad}$ bond energy at the gas−solid interface (∼350 kJ/mol) indicates that the Pt(111)−OH interaction is much weaker than the Pt−O. The weaker interaction of OH_{ad} with the Pt(111) surface supports a high catalytic activity of the OH_{ad} state in the surface electrochemistry of CO_{ad} on Pt(*hkl*) surfaces, in agreement with observations of a very high catalytic activity of Pt(*hkl*) for the electooxidation of CO_b in an alkaline solution.[33] In essence, this proposal invokes one of the oldest concepts in catalysis, the "active site model" (see the very interesting historical review of the active site model for heterogeneous H_2-O_2 oxidation on Pt(111) in the recent paper by Verheij and Hugenschmidt[34] and theoretical aspects of the adsorption and surface chemical reactions at step sites by Hammer and Norskov[35]). The explanation for the remarkable effect of pH on the rate of CO_b oxidation on Pt(111) in the preignition potential is the adsorption of OH_{ad} at defect sites, *which occurs only in alkaline* solution. In acid solution these sites are blocked by anions (spectator species).

The explanation we offer here for the effect of pH on the ignition potential is more speculative than the active site model for the preignition region. The fact that the activation energies determined in both potential regions are basically identical implies that the surface coverage by OH_{ad} is the principal cause of the rapid increase in rate above the ignition potential. At the ignition potential, we propose that the OH_{ad} coverage increases from some nominal value typical of defect concentrations, e.g., $10^{12}-10^{13}$ per cm^2, to a large occupation of terrace sites, e.g., $10^{14}-10^{15}$ per cm^2. For clean Pt(111), i.e., in the absence of CO_{ad}, OH_{ad} nucleation on the (111) terraces becomes thermodynamically favorable in *both* acidic and basic solutions as the potential approaches ca. 0.6 V. The pronounced pH effect on the ignition potential can be understood if we consider an observation made previously[23] and restated here, that for CO oxidation in acid solution in the potential region of 0.7−0.9 V there is only a single-sweep transient current that decays rapidly. The transient current indicates that there is some OH_{ad} adsorbed onto the surface in this potential region, enough to oxidize only a small amount of the "weakly adsorbed" CO_{ad}. Continuous CO oxidation under these conditions, however, is impeded by the much lower surface coverage by OH_{ad} in acid solution than in base solution. While in acid solution there is a competition for the Pt sites between OH_{ad}, CO, and anions from the

supporting electrolyte,[23] in basic solution the surface coverage by OH_{ad} is only limited by the surface coverage of CO_{ad}. Consequently, the CO oxidation kinetics is increased in alkaline solution.

Conclusions

The variation of the adsorption pseudocapacitance with temperature was used to obtain the enthalpy, entropy, and free energies of adsorption of H_{upd} and OH_{ad} on Pt(111) as a function of both pH and the nature of the anion of the supporting electrolyte. It is shown that the heat (enthalpy) of adsorption of hydrogen on Pt(111) at the electrochemical interface is essentially independent of either pH or the nature of the supporting anion. The heat of adsorption has a linear decrease with Θ_{Hupd}, from ~42 kJ/mol at $\Theta_{Hupd} = 0$ ML to ~24 kJ/mol at $\Theta_{Hupd} = 0.66$ ML. The heat of adsorption of OH_{ad} is more sensitive to the nature of the anion in the supporting electrolyte. This is presumably due to coadsorption of the anion and OH_{ad} in electrolytes other than the simple alkali bases. From the isosteric heat of adsorption of OH_{ad} in alkaline solution (~200 kJ/mol) and the enthalpy of formation of $OH^{\bullet}$, we estimated the Pt(111)−OH_{ad} bond energy of 136 kJ/mol. Because this value is much smaller than the Pt−O_{ad} bond energy at a gas−solid interface (~350 kJ/mol), we characterize the OH_{ad} state as a reactive state. It is proposed that the rate of CO_{ad} electrooxidation is dependent on the nature of anions present in the supporting electrolytes. In basic solution the reaction proceeds at low overpotentials (<0.2 V) between the adsorbed states of CO_{ad} and OH_{ad}, the latter forming at low overpotentials selectively at defect sites. In acid solution, however, these sites are not active because they are blocked by specific adsorption of anions: Cl in perchloric acid and bisulfate in sulfuric acid solution.

Acknowledgment. This work was supported by the Assistant Secretary for Conservation and Renewable Energy, Office of Transportation Technologies, Electric and Hybrid Propulsion Division of the U.S. Department of Energy under Contract No. DE-AC03-76SF00098 and by the "Zukunftsoffesive Junge Generation" of the state Baden-Wurttemberg, Germany under Contract No. A00009696. T.J.S. thanks the "Deutscher Akademischer Austauschdienst" (DAAD) for a travel grant.

Glossary

D_{M-H}	metal−hydrogen bond energy
D_{H-H}	dissociation energy for H_2
D_{O-O}	dissociation energy for O_2
D_{M-OH}	metal−OH bond energy
D_{M-O}	metal−O bond energy
E_{RHE}	potential with respect to the reversible hydrogen electrode
$E^0_{O_2/H_2O}$ standard potential for eq 15	$E^0_{OH_{ad}}$standard potential for the adsorption reaction given by eq 11
F	Faraday constant
f	Frumkin interaction parameter; $f = r/(RT)$
$\Delta G_{H_{upd}}$	apparent Gibbs energy of H_{upd}
Δ	$G^{\Theta=0}_{H_{upd}}$apparent Gibbs energy of H_{upd} at $\Theta = 0$
$\Delta G^{\Theta=0.5}_{OH_{ad}}$	apparent Gibbs energy of OH_{ad} at $\Theta = 0.5$
$\Delta G_{OH_{ad}}$	apparent Gibbs energy of OH_{ad}
Δ	$G^0_{O_2/H_2O}$standard Gibbs energy for eq 15
$\Delta H_{H_{upd}}$	apparent enthalpy of adsorption for H_{upd}
$\Delta_f H^0$	standard enthalpy of formation
$\Delta_r H^0$	standard enthalpy of reaction
q^H_{st} isosteric heat of adsorption for H_{upd}	q^{OH}_{st}
isosteric heat of adsorption for OH_{ad}	q^O_{st} isosteric heat of adsorption of O_{ad}
R	gas constant
r	rate of change of $\Delta G_{H_{upd}}$ with $\Theta_{H_{upd}}$
$\Delta S_{H_{upd}}$	apparent entropy of adsorption for H_{upd}
$\Delta_f S^0$	standard entropy of formation
T	temperature of the electrolyte
Θ	partial coverage by H_{upd}
$U_{OH_{ad}}$	potential difference defined by eq 14

References and Notes

(1) (a) Hubbard, A. T.; Ishikawa, R. P.; Katekaru, J. *J. Electroanal. Chem.* **1978**, *86*, 271. (b) Homa, A. S.; Yeager, E.; Cahan, B. D. *J. Electroanal. Chem.* **1983**, *150*, 181. (c) Wagner, F. T.; Ross, P. N. *J. Electroanal. Chem.* **1983**, *150*, 141.

(2) (a) Ocko, B. M.; Wang, J.; Davenport, A.; Isaacs, H. *Phys. Rev. Lett.* **1990**, *65*, 1466. (b) Tidswell, I. M.; Marković, N. M.; Ross, P. N. *Phys. Rev. Lett.* **1993**, *71*, 1601. (c) Villegas, I.; Weaver, M. J. *J. Chem. Phys.* **1994**, *101*, 1648. (d) Magnussen, O. M.; Wiechers, J.; Behm, R. J. *Surf. Sci.* **1993**, *289*, 139. (e) Moeller, F. A.; Magnussen, O. M.; Behm, R. J. *Phys. Rev. Lett.* **1996**, *77*, 107.

(3) Marković, N. M.; Gasteiger, H. A.; Ross, P. N. *J. Phys. Chem.* **1995**, *99*, 3411.

(4) Marković, N. M.; Sarraf, S. T.; Gasteiger, H. A.; Ross, P. N. *J. Chem. Soc., Faraday Trans.* **1996**, *92*, 3719.

(5) (a) Marković, N. M.; Grgur, B. N.; Ross, P. N. *J. Phys. Chem. B* **1997**, *101*, 5405. (b) Grgur, B. N.; Marković, N. M.; Ross, P. N. In preparation.

(6) (a) Marković, N. M.; Gasteiger, H. A.; Ross, P. N. *J. Phys. Chem.* **1996**, *100*, 6715. (b) Marković, N. M.; Gasteiger, H. A.; Ross, P. N. *J. Electrochem. Soc.* **1997** *144*, 1591. (c) Grgur, B. N.; Marković, N. M.; Ross, P. N. *Can. J. Chem.* **1997**, *75*, 1.

(7) (a) Zolfaghari, A.; Chayer, M.; Jerkiewicz, G. *J. Electrochem. Soc.* **1997**, *144*, 3034. (b) Zolfaghari, A.; Jerkiewicz, G. In *Electrochemical Surface Science of Hydrogen Adsorption and Adsorption*; Jerkiewicz, G., Marcus, P., Eds.; The Electrochemical Society: Pennington, NJ, 1997; PV97-16.

(8) Wagner, F. T.; Ross, P. N. *J. Electroanal. Chem.* **1988**, *250*, 301.

(9) (a) For acid solution, see the following. Clavilier, J. *J. Electroanal. Chem.* **1980**, *107*, 211. (b) For alkaline solution, see the following. Lamy, C.; Leger, J. M.; Clavilier. J. *J. Electroanal. Chem.* **1982**, *135*, 321. Marković, N. M.; Avramov-Ivić, M. L.; Marinković, N. S.; Adzić, R. R. *J. Electroanal. Chem.* **1991**, *312*, 115.

(10) Conway, B. E.; Angerstein-Kozlowska, H.; Sharp, W. B. *J. Chem. Soc., Faraday Trans. 1* **1978**, *74*, 1373.

(11) Conway, B. E.; Angerstein-Kozlowska, H.; Dhar, H. P. *Electrochim. Acta* **1974**, *19*, 455.

(12) Gileadi, E. *Electrode Kinetics for Chemists, Chemical Engineers, and Materials Scientists*; VCH: New York, 1993.

(13) Marković, N.; Ross, P. N. *J. Electroanal. Chem.* **1992**, *330*, 499.

(14) Gasteiger, H. A.; Marković, N. M.; Ross, P. N. *Langmuir* **1996**, *12*, 1414.

(15) Ross, P. N. *Chemistry and Physics of Solid Surfaces IV*; Vanselow, R., Howe, M., Eds.; Springer Series in Chemical Physics; Springer-Verlag: Berlin, 1980; Vol. 20, Chapter 8.

(16) (a) Wagman, D. D.; Evans, W. H.; Parker, V. B.; Schumm, R. H.; Halow, I.; Bailey, S. M.; Churney, K. L.; Nuttall, R. L. The NBS Tables of Chemical Thermodynamic Properties. *J. Phys. Chem. Ref. Data* **1982**, *11* (Suppl. 2). (b) Lupis, C. H. P. *Chemical Thermodynamics of Materials*; North-Holland: New York, 1983; p 33.

(17) Fromm, E.; Mayer, O. *Surf. Sci*. **1978**, *74*, 259.

(18) Bond, G. C. *Heterogeneous Catalysis: Principles and Applications*; Clarendon Press: Oxford, 1974.

(19) Lee, W. T.; Ford, L.; Blowers, P.; Nigg, H. L.; Masel, R. I. *Surf. Sci.* **1998**, *416*, 141.

(20) Conway, B. E. *Progress in Surface Science*; Davison, S., Ed.; Pergamon: Fairview Park, New York, 1984; Vol. 16, pp 1−138.

(21) (a) You, H.; Zurawski, D. J.; Nagy, Z.; Yonco, R. M. *J. Chem. Phys.* **1994**, *100*, 1. (b) You, H.; Nagy, Z. *Physica B* **1994**, *1*, 187.

(22) Tidswell, I. M.; Marković, N. M.; Ross, P. N. *J. Electroanal. Chem*. **1994**, *376*, 119.
(23) Marković, N. M.; Grgur, B. N.; Lucas, C. A.; Ross, P. N. *J. Phys. Chem.* **1999**, *103*, 487.
(24) (a) Christmann, K.; Ertl, G. *Surf. Sci.* **1976**, *41*, 365. (b) Christmann, K. In *Electrocatalysis*; Lipkowski, J., Ross, P. N., Eds.; Wiley-VCH: New York, 1998; pp 1−41.
(25) Breiter, M. W. Ann. N.Y. Acad. Sci. **1963**, *101*, 709. Breiter, M. W. *Electrochim. Acta* **1962**, *7*, 25.
(26) Protopopoff, E.; Marcus, P. *J. Chim. Phys.* **1991**, *88*, 1423.
(27) Smoluchowski, K. *Phys. Rev.* **1941**, *60*, 107.
(28) Clavilier, J.; Rodes, A.; El Achi, K.; Zamakhchari, M. *J. Chim. Phys.*. **1991**, *88*, 1291.
(29) Marković, N. M.; Marinković, N. S.; Adzić, R. R. *J. Electroanal. Chem*. **1988**, *214*, 309; **1991**, *314*, 289.
(30) Ross, P. *J. Chim. Phys.* **1991**, *88*, 1353.
(31) Wandelt, K. *Appl. Surf. Sci.* **1997**, *111*, 1.
(32) Alnot, M.; Eberhardt, J.; Barnard, J. *Surf. Sci.* **1989**, *208*, 285.
(33) Marković, N. M.; Climent, V.; Ross, P. N. Manuscript in preparation.
(34) Verheij, L. K.; Hugenschmidt, M. B. *Surf. Sci.* **1998**, *416*, 37.
(35) Hammer, B.; Norskov, J. K. In *Chemisorption and reactivity on supported clusters and thin films*; Lambert, R., Pacchioni, G., Eds.; Kluwer Academic Publisher: Dordrecht, 1997.